Modelisation and Numerical Methods for Hot Plasmas

Talence, October 14, 2015

Physics of Laser-Plasma Interaction and Shock Ignition of Fusion Reactions

V. T. Tikhonchuk, A. Colaïtis, A. Vallet, E. Llor Aisa, G. Duchateau, Ph. Nicolaï, X. Ribeyre

Centre Laser Intenses et Applications
University of Bordeaux, CNRS, CEA

Outline

1. Principles of Inertial Confinement Fusion and shock ignition scheme
2. Ignition condition with a shock
3. Shock amplification in the imploding shell
4. Laser plasma interactions and generation of a strong shock with hot electrons
5. Integrated simulations of shock ignition
6. Experiments on the strong shock generation

Principles of the Inertial Confinement Fusion

The process of ICF consists of two steps

- compress the fuel to densities 200-300 g/cc
- heat a small part of the fuel to the ignition temperature T_h ~ 7-10 keV

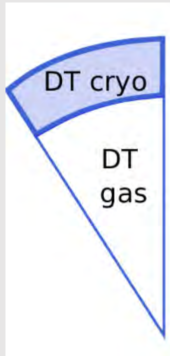

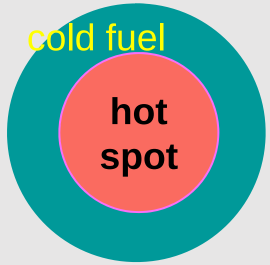

In the standard ICF schemes these two goals are achieved the laser pulse by temporal profiling

Ablation pressure ~ 100 Mbar

Implosion velocity ~ 300 – 350 km/s

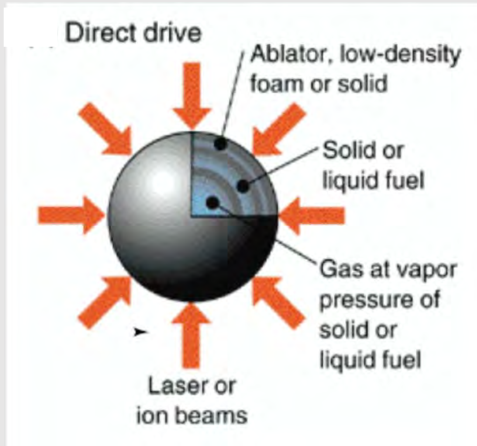

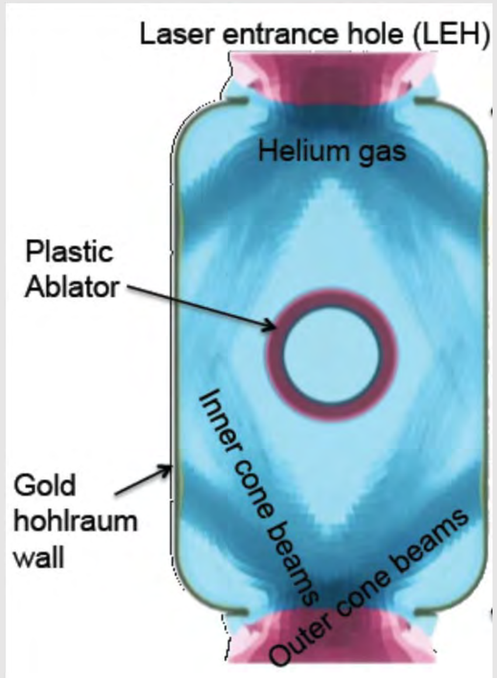

Controversy:

Ignition requires high implosion velocity – shell instability $T_h \sim u_{imp}^{1.25}$

High gain requires low implosion velocity $G \sim u_{imp}^{-1.25}$

Shock Ignition scheme

Alternative ignition schemes separate the implosion and ignition phases: the ignition is achieved with a special intense laser spike

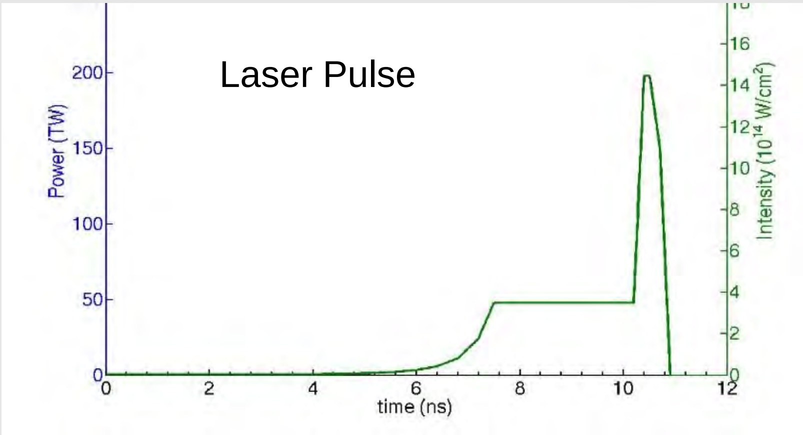

Low implosion velocity 250-300 km/s

- **More stable implosion**
- **Lower laser energy**
- **Accessible with existing installations NIF & LMJ**

The shock ignition scheme is selected for the European ICF project HiPER

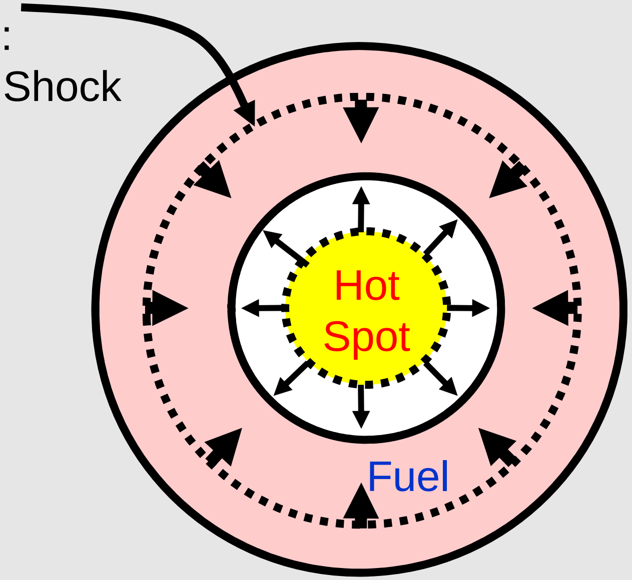

Review on alternative ignition schemes:
Nuclear Fusion 54, No. 5 (2015)

Shcherbakov V.A. Sov. J. Plasma Phys (1983)
Betti R. et al. PRL 98 (2007); Ribeyre X. et al PPCF (2009)

Hydrodynamics of implosion and ignition

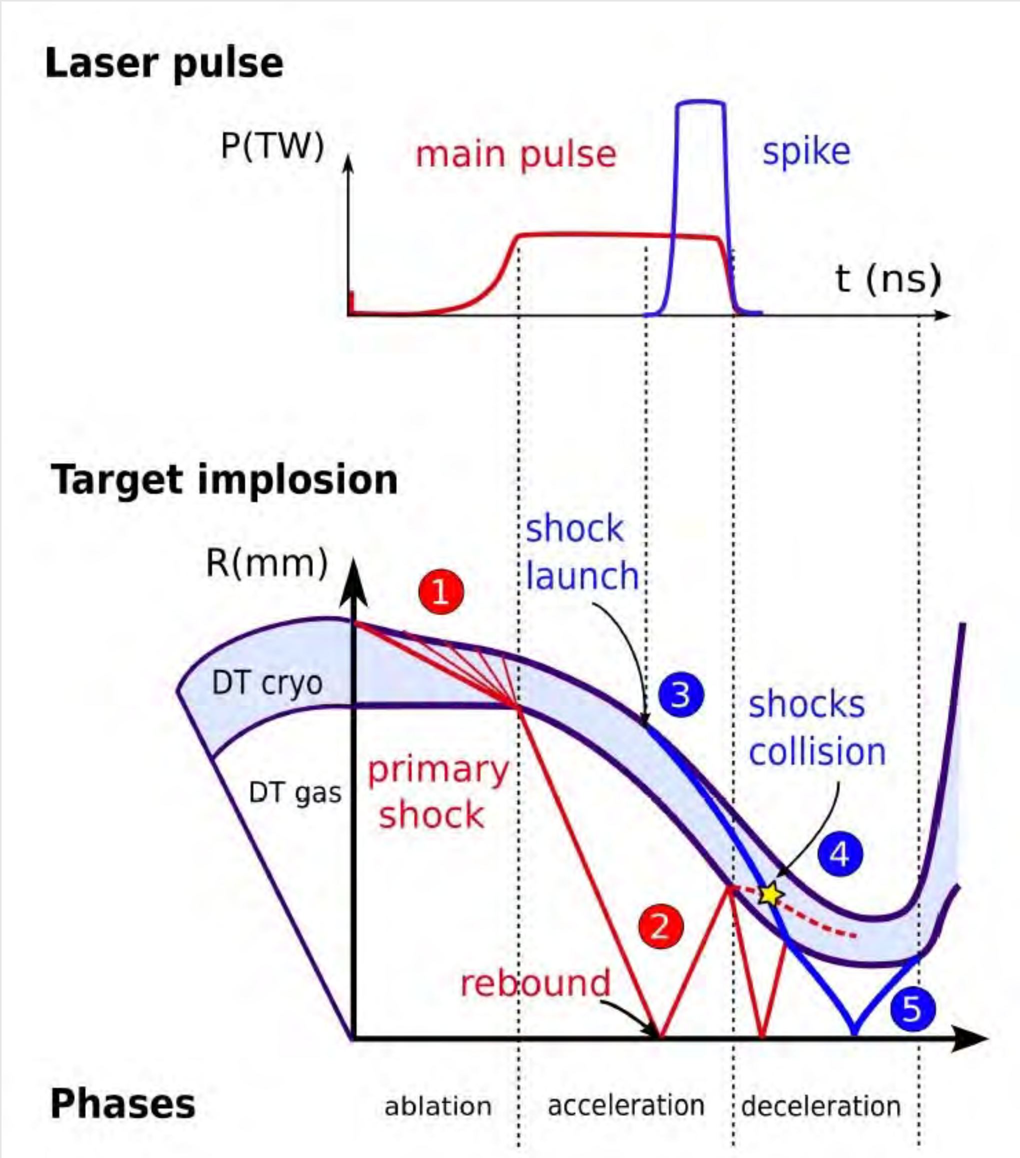

Sequence of processes in the shock ignition scheme are controlled by the time and the amplitude of the laser spike

1. **Shell compression**
2. **Shell acceleration**
3. **Shock launch**
4. **Shell deceleration and Shock collision**
5. **Shock propagation through the hot-spot and ignition**

Physical issues related to shock ignition scheme

We discuss here the processes occurring from the time of spike launch to ignition: $\Delta t \sim 1$ ns

Laser plasma interaction and generation of a strong shock

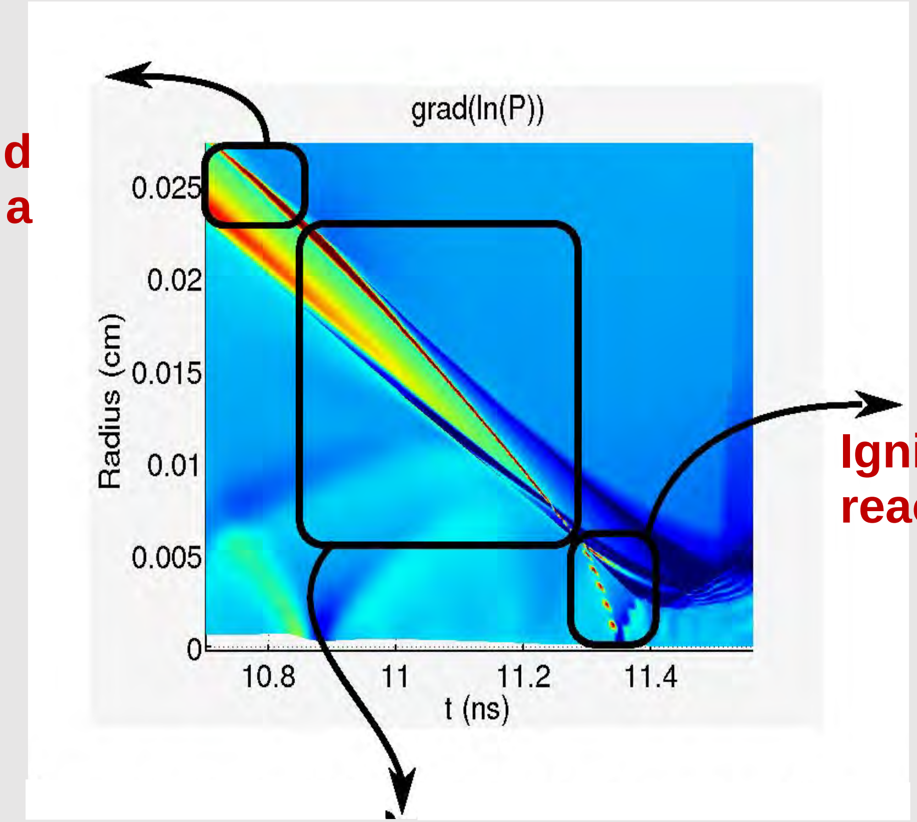

Ignition of the fusion reactions with a shock

Propagation of the shock across the shell and pressure amplification

Hot spot ignition with a strong shock

Shock crossing the hot spot should rise its temperature to ignition: Δt ~ 0.2 ns

Shock entering in the hot spot **Moment of ignition**

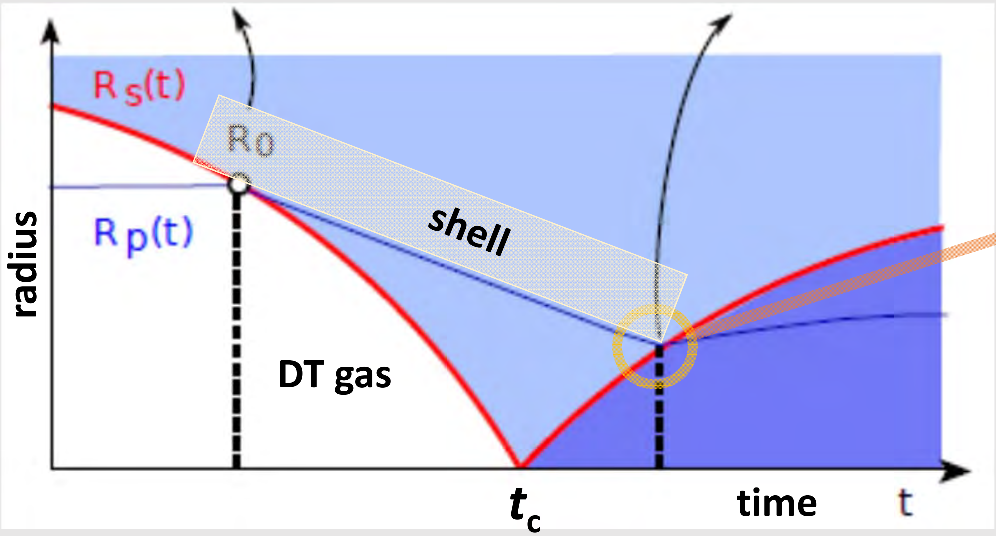

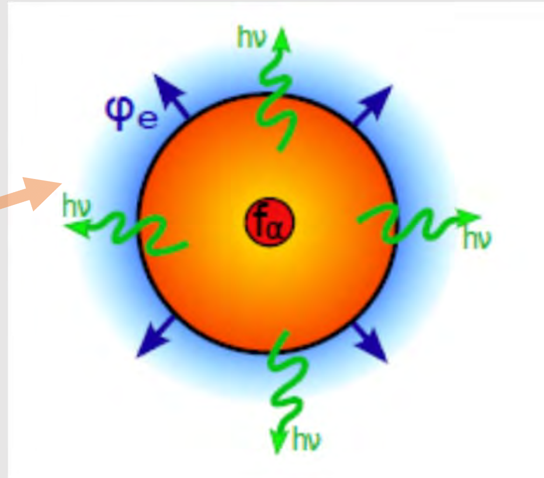

Shock propagation is described by the self-similar solution

$$R_s(t) \propto |t - t_c|^\alpha \qquad \alpha = 0.688$$

$$f_\alpha W_\alpha > W_{Brem} + W_e$$

Power balance at the shock breakout
f_a – fraction of absorbed α-particles

Guderley V.G. Luftfahrforschung (1942)

Ignition condition in the hot spot

Ignition condition relates the shock velocity and the hot spot areal density

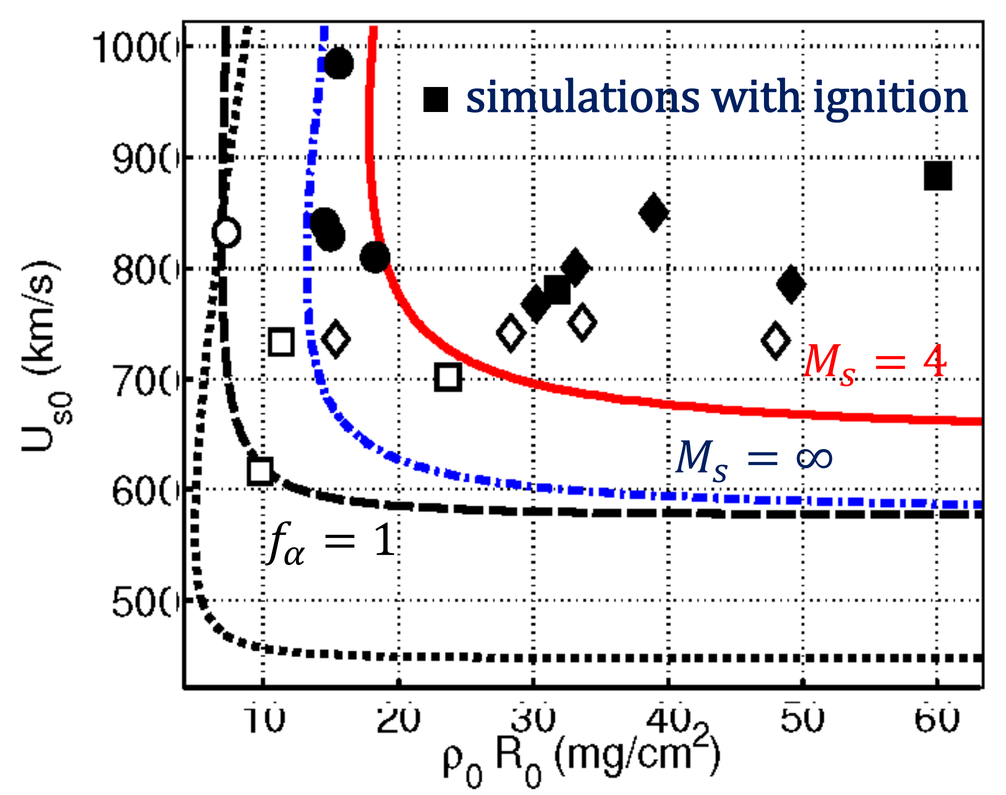

Hydrodynamic simulations for a standard HiPER target confirm these estimates

Ribeyre X. Phys. Plasmas (2011)

Factors to be accounted for:

- **Temperature dependence of the reaction rate**
- **α-particle losses from the core**
- **Initial core pressure (finite shock Mach number)**

Ignition threshold for the hot spot radius of 50 μm corresponds to the shock pressure of 30 Gbar

$$p_s \cong 0.76\, \rho_0 U_{s0}^2$$

To compare with the achieved ablation pressures of 100 Mbar

Shock pressure amplification > 100× is needed

Shock pressure amplification: Δt ~ 0.3 ns

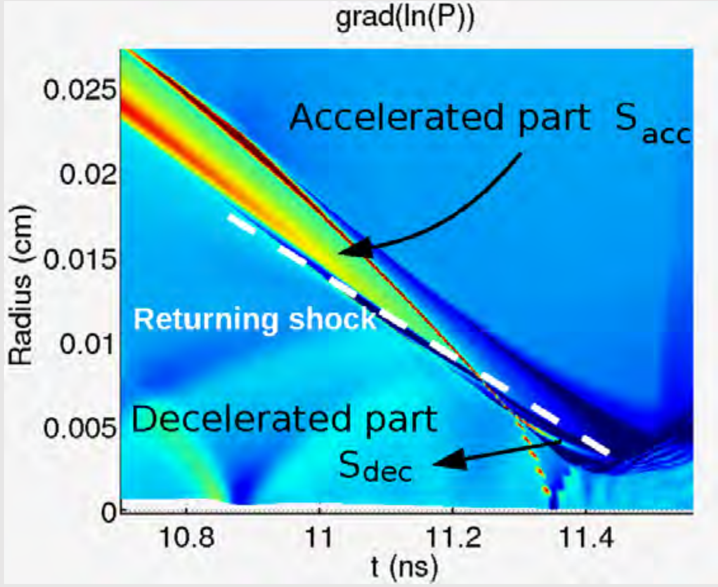

The total ignitor shock pressure amplification in the imploding shell contain three contributions:

- **the shell implosion** χ_{imp}
- **the shock amplification in the shell** χ_{shell}
- **the collision with the diverging shock** χ_{coll}

$$p_{sf}/p_{si} = \chi = \chi_{imp}\chi_{shell}\chi_{coll}$$

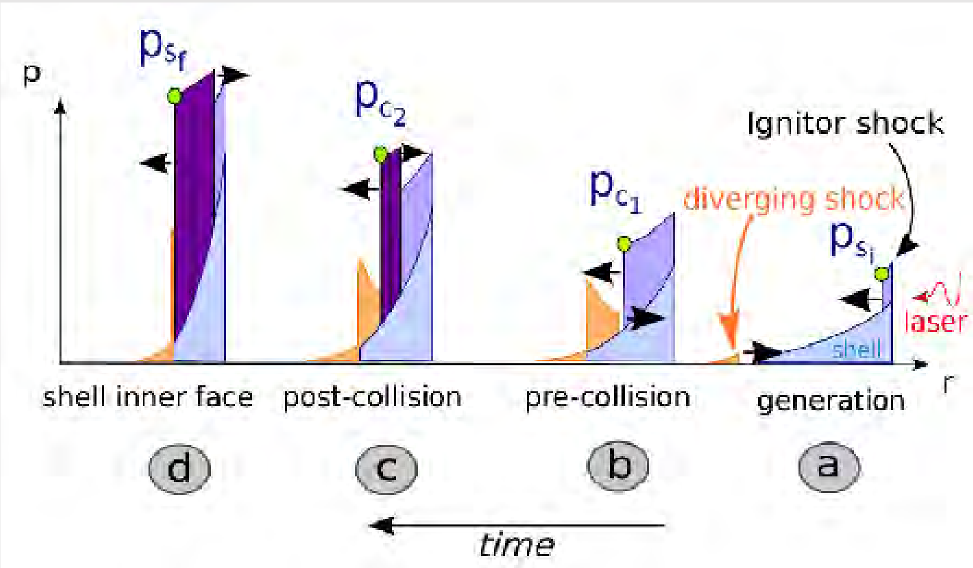

- **Shell pressure amplification is χ_{imp} = 15 during the time of shell deceleration**
- **Shock amplitude increases as the shell is decelerated χ_{shell} = 2**
- **Pressure amplification in the shock collision χ_{coll} ~ 2 - 3**

Vallet A. PhD thesis, 2014

Total shock pressure amplification

Numerical simulation for the HIPER target design: comparison with the analytical model

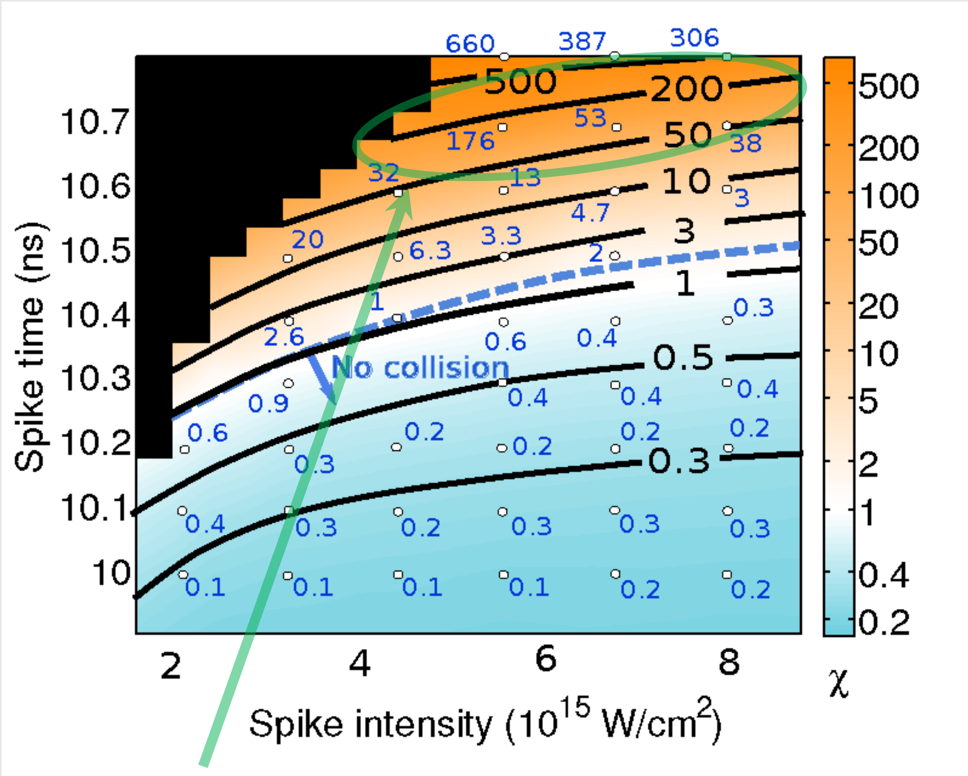

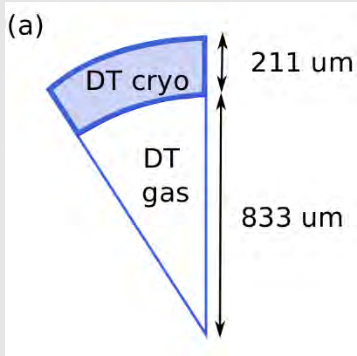

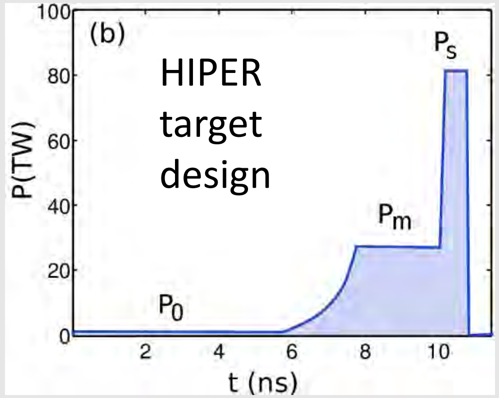

- **Optimal amplification χ > 100 can be achieved in a time window of 200 ps**
- **Laser intensities about 10^{16} W/cm^2 are required**
- **Nonlinear laser plasma interactions need to be accounted for**

Strong shock generation with lasers

Assuming the shock amplification factor χ ~ 100 one need to generate shock pressure > 300 Mbar, the corresponding laser intensities ~ 10 PW/cm^2 and large scale plasma corona imply strongly nonlinear laser plasma interaction

The questions are:

- **What is the overall absorption efficiency?**
- **Where does the absorption take place?**
- **Which processes contribute to absorption?**
- **Which processes are the most detrimental?**

High laser intensities 1 – 10 PW/cm^2, high plasma temperatures T ~ 2 – 5 keV, large scale length L ~ 300 µm require kinetic (PIC) simulations
Simulation time ~ tens of ps

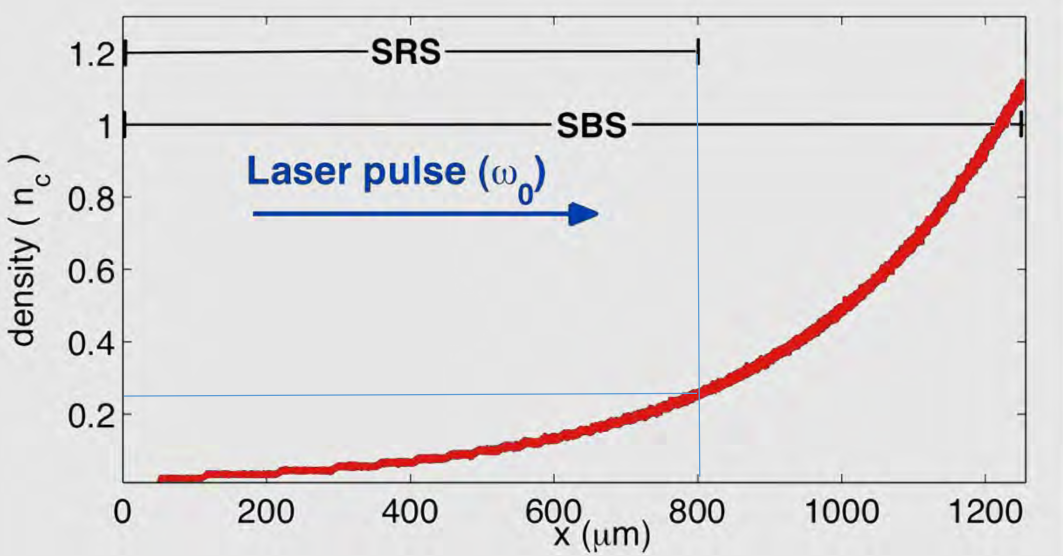

O. Klimo et al. Plasma Phys Contr. Fusion, 2011

SRS and TPD

Stimulated Raman scattering (SRS) and Two plasmon decay (TPD) are most dangerous parametric instabilities as they produce electron plasma waves strongly coupled to electrons

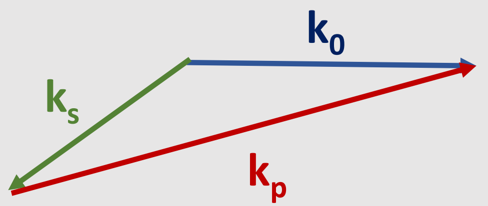

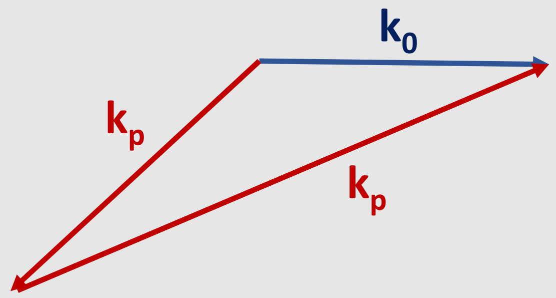

SRS corresponds to excitation of a plasma wave with a narrow spectrum in the density region $n_e < \frac{1}{4} n_c$
Growth rate: $\gamma_{SRS} = {}^{1}/_{4}\, k_p v_{\mathrm{osc}}$
Threshold:
$I_{thSRS} = 99.5 L_n^{-4/3} \lambda_{\mathrm{las}}^{-2/3}$ PW/cm²

TPD corresponds to excitation of two plasma waves with a broad spectrum in the density region $n_e \approx \frac{1}{4} n_c$
Growth rate: $\gamma_{TPD} = {}^{1}/_{4}\, k_p v_{\mathrm{osc}}$
Threshold:
$I_{thTPD} = 8.2 T_{\mathrm{keV}} L_n^{-1} \lambda_{\mathrm{las}}^{-1}$ PW/cm²

The competition between these instabilities depend on the plasma temperature and density profile

Laser plasma interaction in a target corona

Large scale kinetic simulations in a plasma corona show the dramatic change of the interaction regime at the laser intensities 2-3 PW/cm^2.

Two major effects:

- ❑ **Stimulated Raman scattering (SRS)**
- ❑ **Generation of hot electrons**

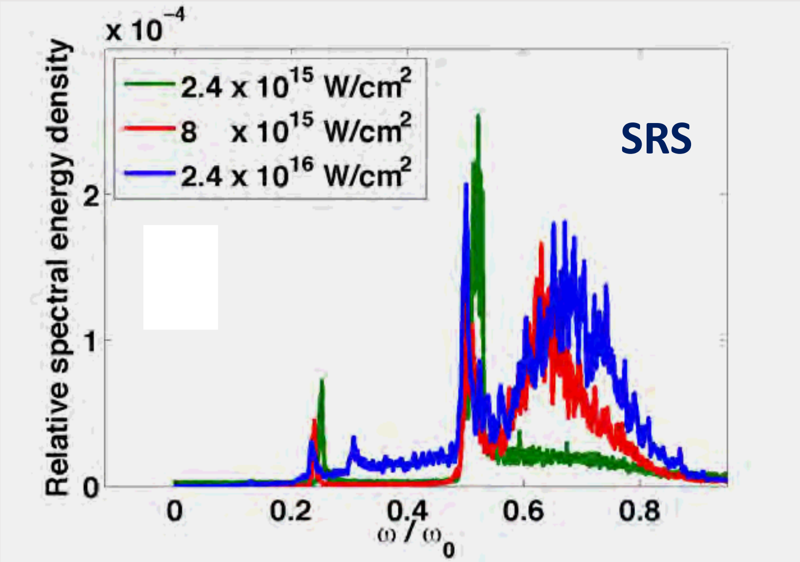

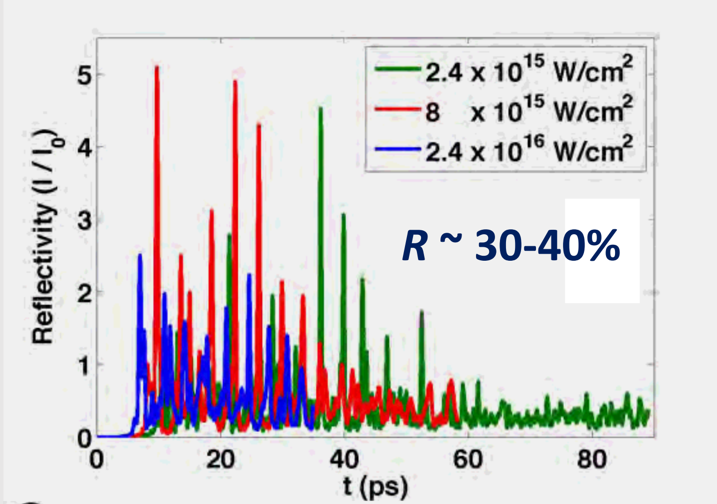

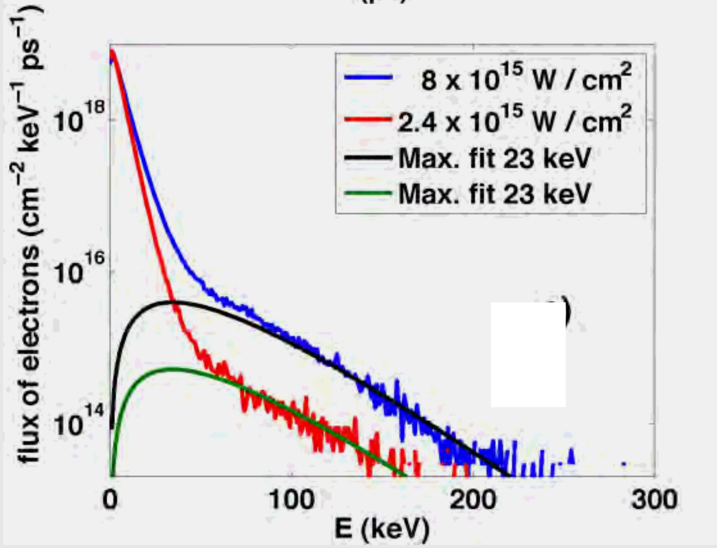

Hot electrons with a temperature ~ 30-40 keV are carrying up to 30% of the energy flux

O. Klimo et al, PPCF 2013

Cavity formation in two dimensional simulations

Cavity formation is confirmed in 2D simulations. Small scale electromagnetic cavities are created near the quarter of critical density
They lead to electron heating and quenching TPD by creating a dynamic phase plate

Poynting vector inside one cavity

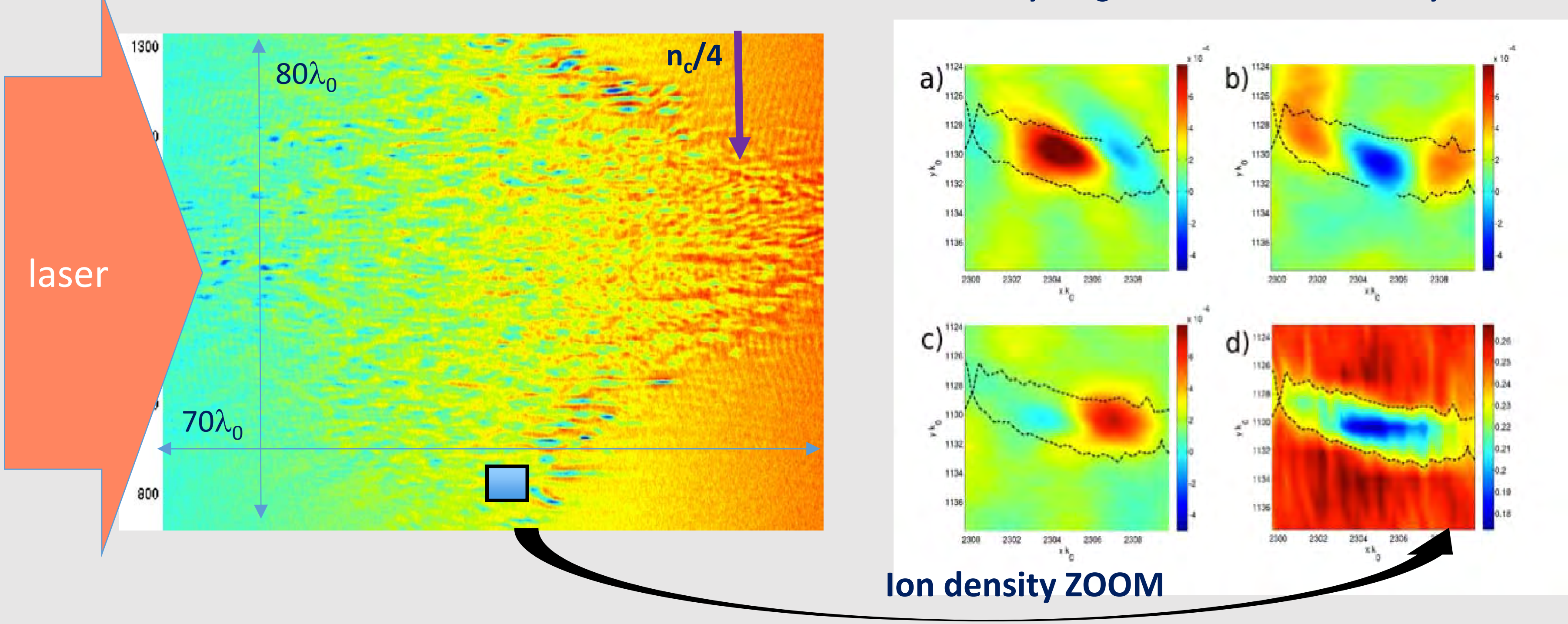

Boiling plasma: electromagnetic fields trapped in the cavities with density modulations
~ 40% accelerate electrons

C. Riconda et al, Phys Plasmas 2013
S. Weber et al, Phys Rev E 2014

Pressure generation with hot electrons

The laser driven ablation pressure is limited by the low critical density and low energy flux

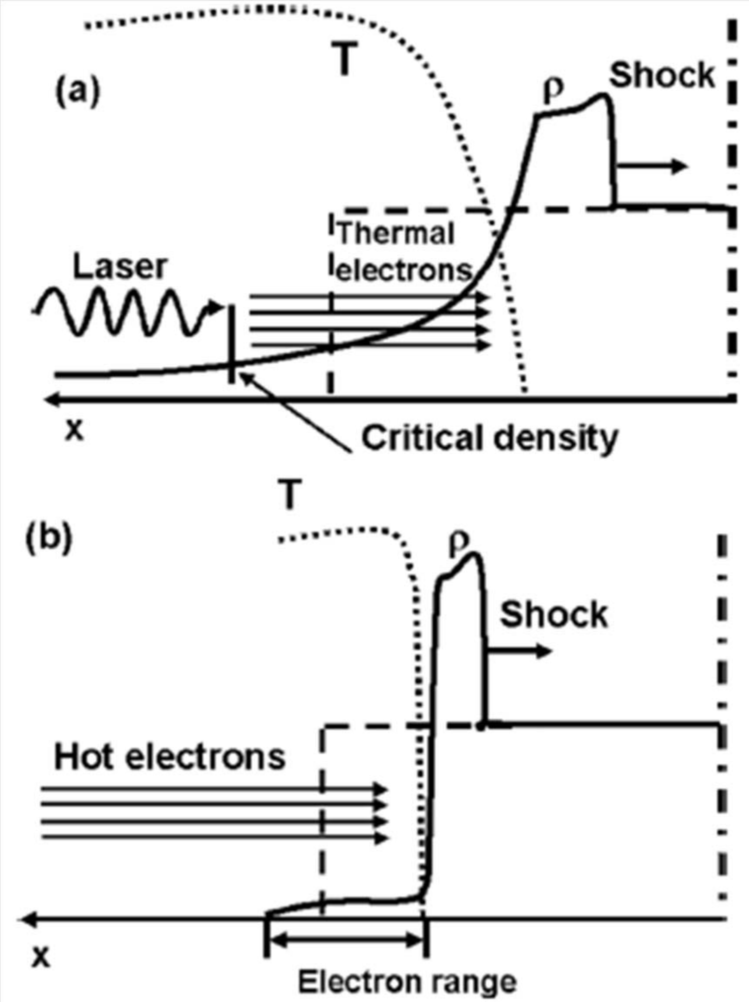

Guskov et al, Phys Rev Lett 2012

A stationary process: constant ablation rate and pressure

Laser absorption
$r < r_c << r_{solid}$
$r_c = 0.03$ g/cm^2
at 0.35 µm

$$\dot{m}_{abl} \cong \rho_c c_s \approx \rho_c^{2/3} I_{abs}^{2/3}$$

$$P_{abl} \cong \rho_c^{1/3} I_{abs}^{2/3}$$

Electron beam absorption
$\rho \approx \rho_{solid}$

$$\rho R_s \cong 0.276 A_t Z_t^{-8/9} \varepsilon_{e\,\mathrm{MeV}}^{5/3} \ \mathrm{g/cm^2}$$

The electron beam deposes its energy in a high density ~ 5 – 10 g/cc – large gain

Shock formation with monoenergetic electrons

In difference from the laser driven absorption, the hot electron drive is limited by the time of formation of rarefaction wave

A non-stationary process: constant ablated mass

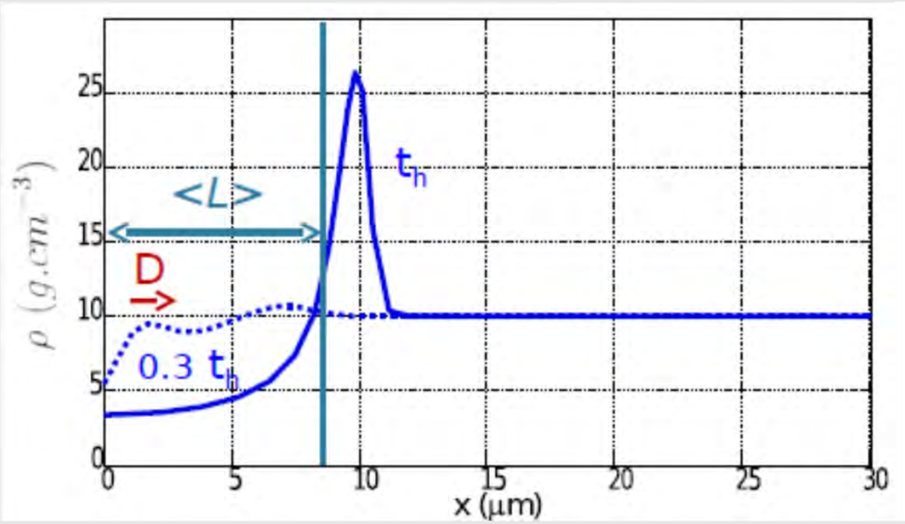

Length of the energy deposition zone is defined by the electron range

$$L \cong \rho R_s / \rho_0$$

$$\rho R_s \cong 0.276 A_t Z_t^{-8/9} \varepsilon_{e\,\mathrm{MeV}}^{5/3}\ \mathrm{g/cm^2}$$

Deposited energy defines the characteristic plasma velocity and beam loading time

$$W \cong I_b t_h / L \cong \rho_0 D^2 \quad + \quad t_h \cong L / D \quad \rightarrow \quad D \cong (I_b / \rho_0)^{1/3}$$

Guskov et al, Phys Rev Lett 2012

Numerical simulations of the pressure generation

Numerical simulations of the interaction of intense monoenergetic electron beam with a dense plasma confirm the model estimates

I_b = 10 PW/cm^2 ε_e = 100 keV

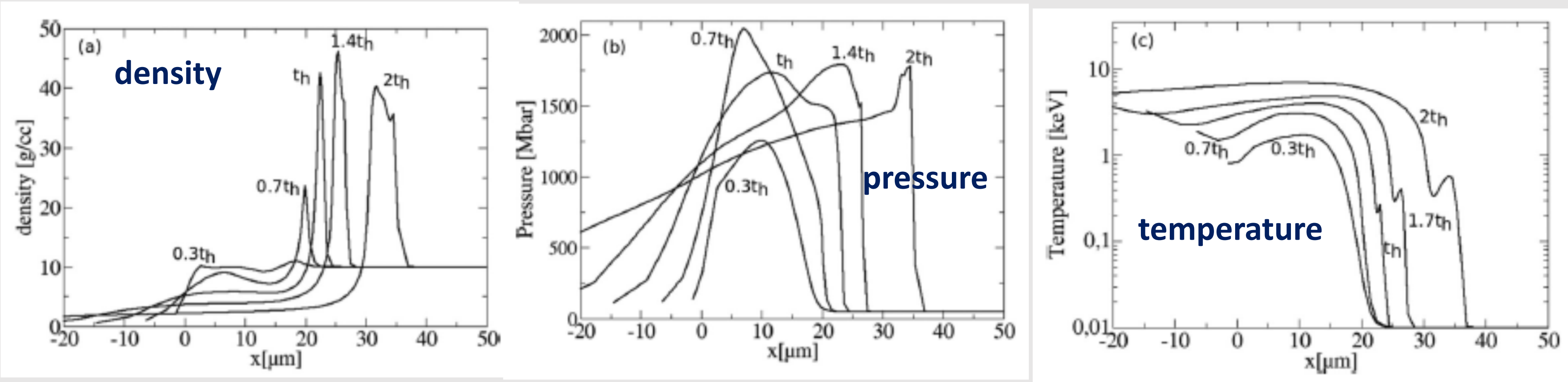

- **Formation of the rarefaction wave**
- **Formation of a strong density compression and a blast wave**
- **Homogeneous heating of expanding plasma**
- **No heat wave precursor**

Ribeyre et al, Phys Plasmas 2013

Shock generation with Maxwellian electron beams

Position and amplitude of the shock wave generation with a beam having a broad energy distribution are defined by its average stopping range and total intensity:

$$\rho R_s \cong 0.276 A_t Z_t^{-8/9} \varepsilon_{e\mathrm{MeV}}^{5/3}\ \mathrm{g/cm}^2$$

$$\langle \rho R_s \rangle \cong \frac{\int d\varepsilon \sqrt{\varepsilon}\, \rho R_s(\varepsilon) f_e(\varepsilon)}{\int d\varepsilon \sqrt{\varepsilon}\, f_e(\varepsilon)} \approx 2.65 R_s(T)$$

Monoenergetic beam with an energy ε_e has the stopping power equation to the average stopping power of a Maxwellian beam with the temperature $T_{\mathrm{eqv}}=0.56\varepsilon_e$

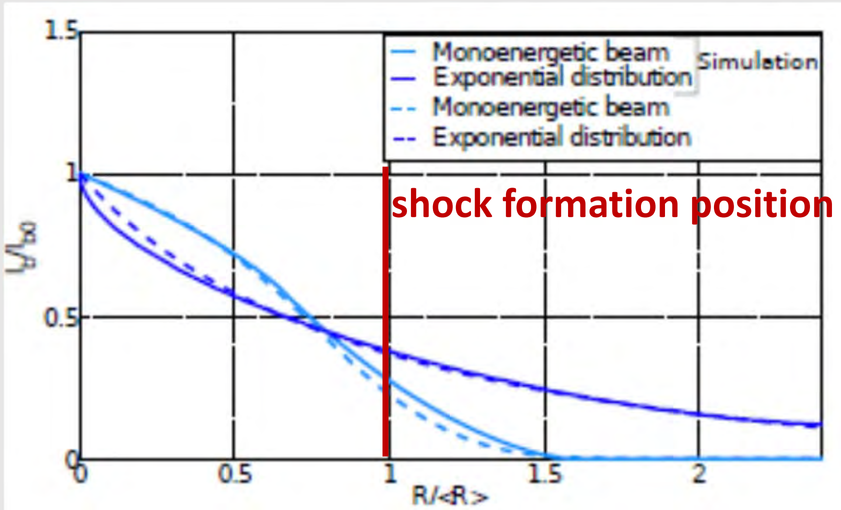

- **Less energy deposited in the post-shock zone**
- **Strong preheat of the pre-shock zone**

Shock generation with a Maxwellian electrons: preheat

A monoenergetic electron beam with ε = 50 keV has stopping range of 5 μm
Same stopping range has a Maxwellian electron beam with T_h = 25 keV

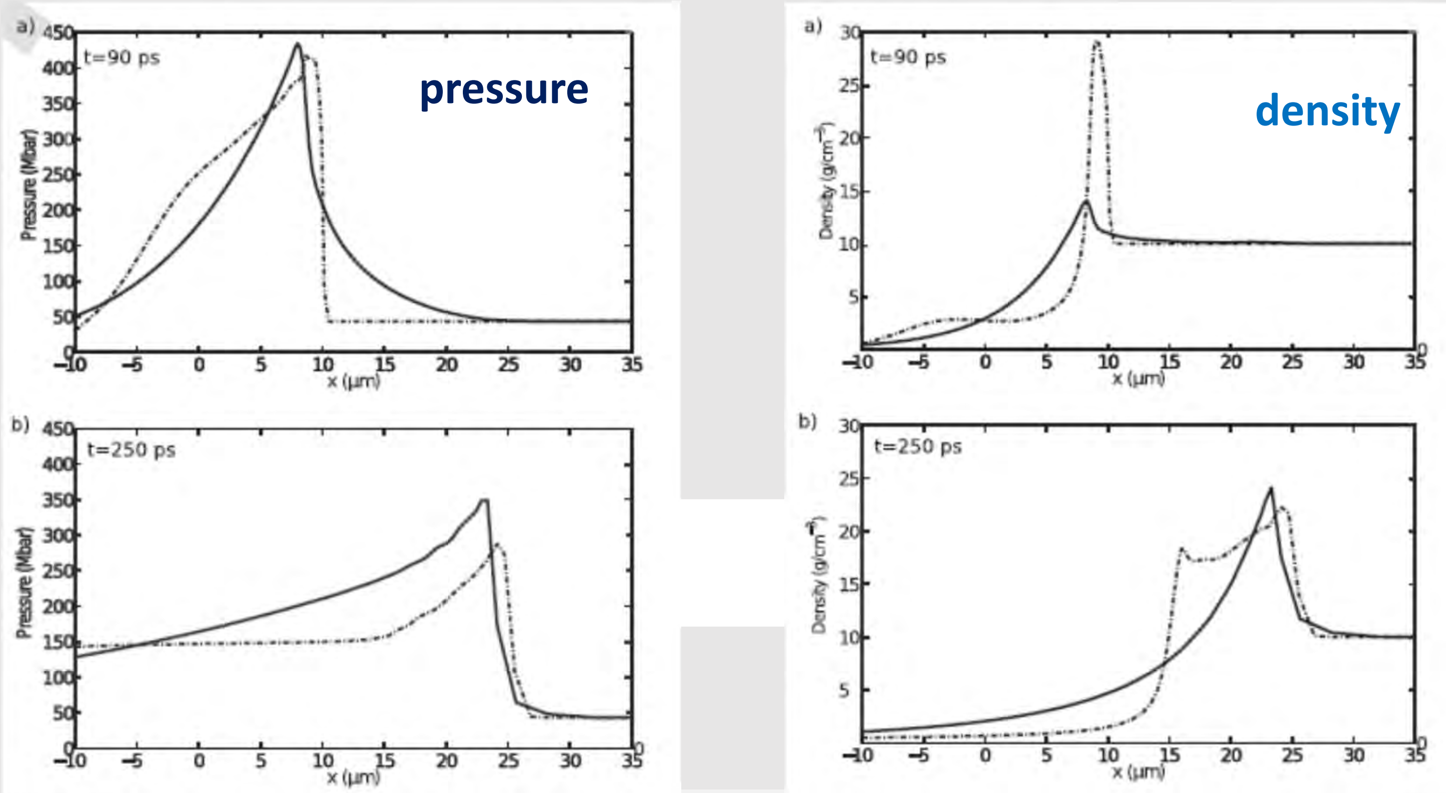

$$I_b = 1\,\text{PW/cm}^2,\ \varepsilon_e = 50\ \text{keV},\ T_h = 25\ \text{keV},\ \rho_0 = 10\,\text{g/cm}^3$$

The same pressure BUT a much smaller shock strength because of the preheat
That makes the process shock formation less efficient

E Llor Aisa et al, Phys Plasmas 2015

Shock generation by electrons in a thin shell

The HiPER shell irradiated with a Maxwellian electron beam at 10.2 ns

$$I_b = 1\,\mathrm{PW/cm^2},\, T_h = 30\,\mathrm{keV},\;\; \rho_0 \Delta x = 37\,\mathrm{m}g/\mathrm{cm}^2 \quad \langle R_s \rangle \cong 5.3\,\mathrm{m}g/\mathrm{cm}^2$$

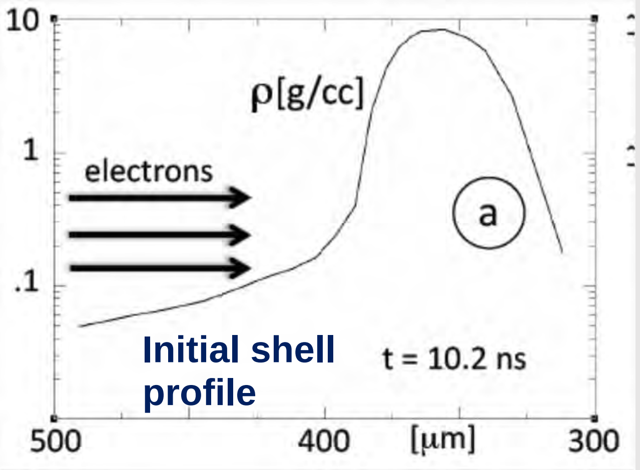

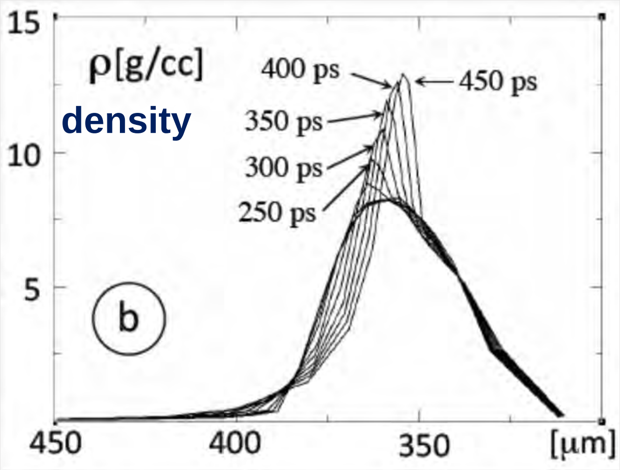

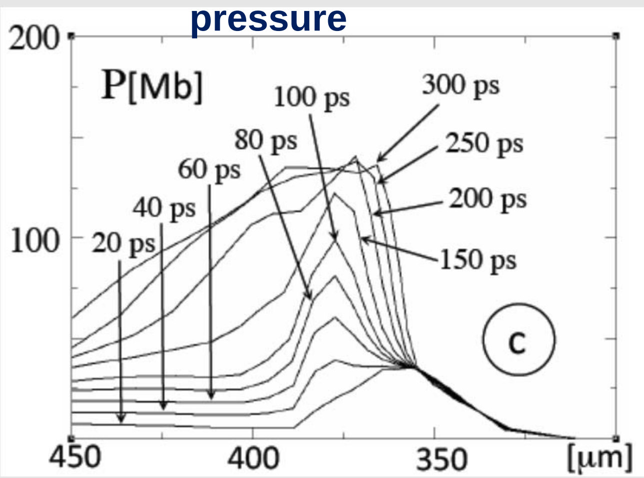

The shock formed at the top of the density profile is incomplete – the pressure is 3 times smaller than expected

Preheat is dangerous: energetic electrons may explode a thin shell

Nicolai et al, Phys Rev E 2014

Laser energy deposition in ICF codes: ray tracing

The laser energy deposition in standard hydrocodes is calculated with the ray tracing technique: application of the geometrical optics to the stationary monochromatic Maxwell's equations

$$E_{\text{las}}(\vec{r}) = u(\omega, \vec{r})\, e^{i\varphi(\vec{r})}$$

$$\Delta u + k_0^2 \epsilon(\omega, \vec{r}) u = 0$$

$$\varphi(\vec{r}) = \varphi(r_\parallel) + i\varphi_a(r_\parallel)$$

Ray centroid Absorption/gain

$$d\vec{r}/d\tau = \vec{p}$$

$$d\vec{p}/d\tau = {}^1/_2\, \nabla\epsilon(\omega, \vec{r})$$

$$dP/d\tau = -\kappa P$$

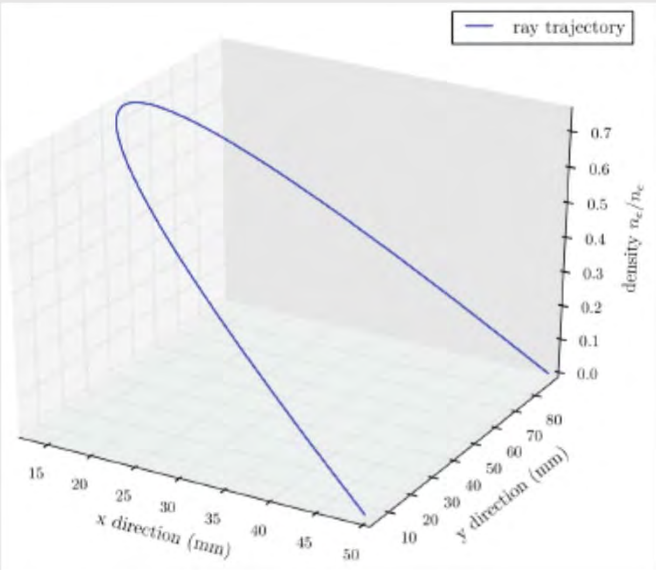

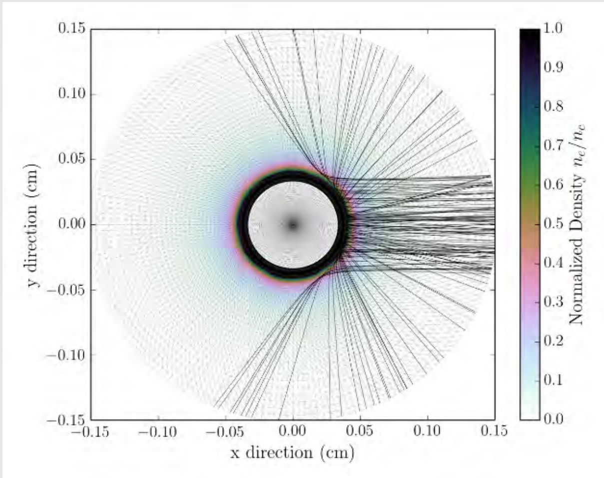

Many rays are needed to describe each laser beam However, this method does not account for diffraction and nonlinear effects

T.B. Kaiser et al, PRE 2000

Towards advanced ICF modelling: thick ray model

New approach of paraxial complex geometrical optics describes the laser intensity in corona and takes into account the cross beam energy transfer, the ponderomotive force, excitation of parametric instabilities and hot electron generation

$$E_{\text{las}}(\vec{r}) = A(\vec{r})\, e^{i\varphi(\vec{r})}$$

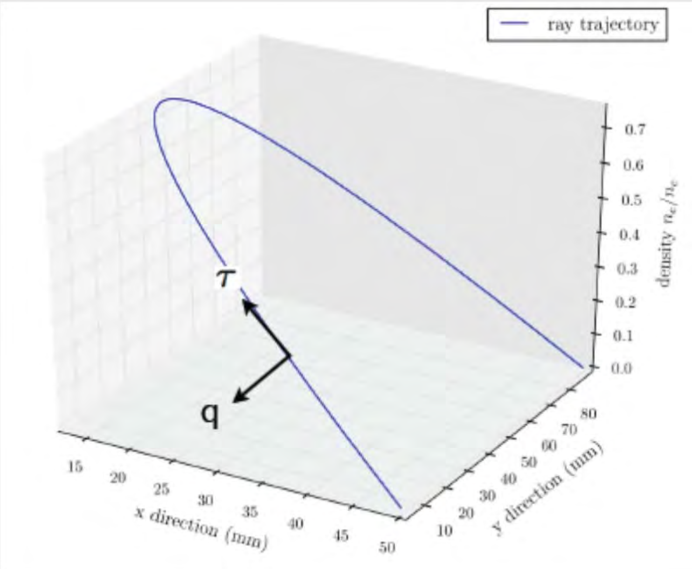

$$\varphi(\vec{r}) = \varphi(r_{\parallel}) + \frac{1}{2} B_{ij} r_{\perp i} r_{\perp j}$$

Ray centroid — Ray curvature/width

Beam width $w(\tau) = \sqrt{2/k_0 \mathrm{Im} B(\tau)}$

Beam curvature $\rho(\tau) = \sqrt{\epsilon_c'}/\mathrm{Re}B(\tau)$

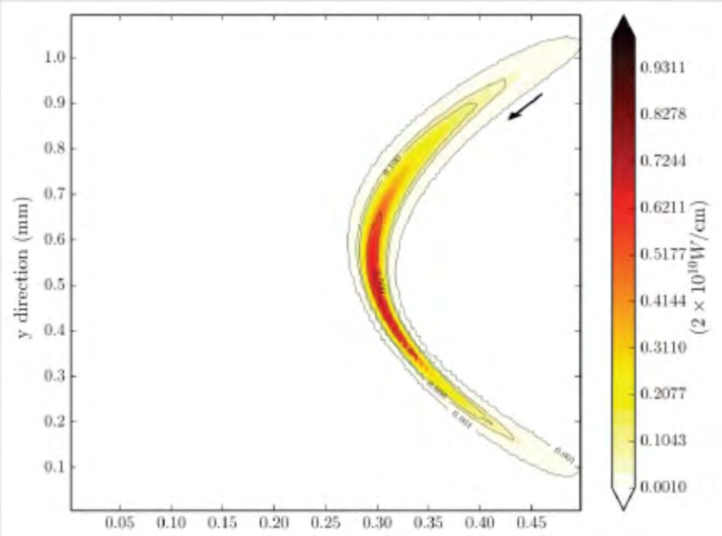

Wave front equation in the ray reference frame

$$B^2 + \frac{dB}{d\tau} = -\frac{3}{4\epsilon}\left(\frac{d\epsilon}{dq}\right)^2 + \frac{1}{2}\frac{d^2\epsilon}{dq^2}$$

Y A Kravtsov, N A Zhu, *Theory of Diffraction*, Oxford 2010
A Colaitis et al, PRE 2014

PCGO model of laser resonance absorption

The model describes the collisional absorption and the hot electron generation due to the resonance absorption of each laser beamlet

Resonance absorption

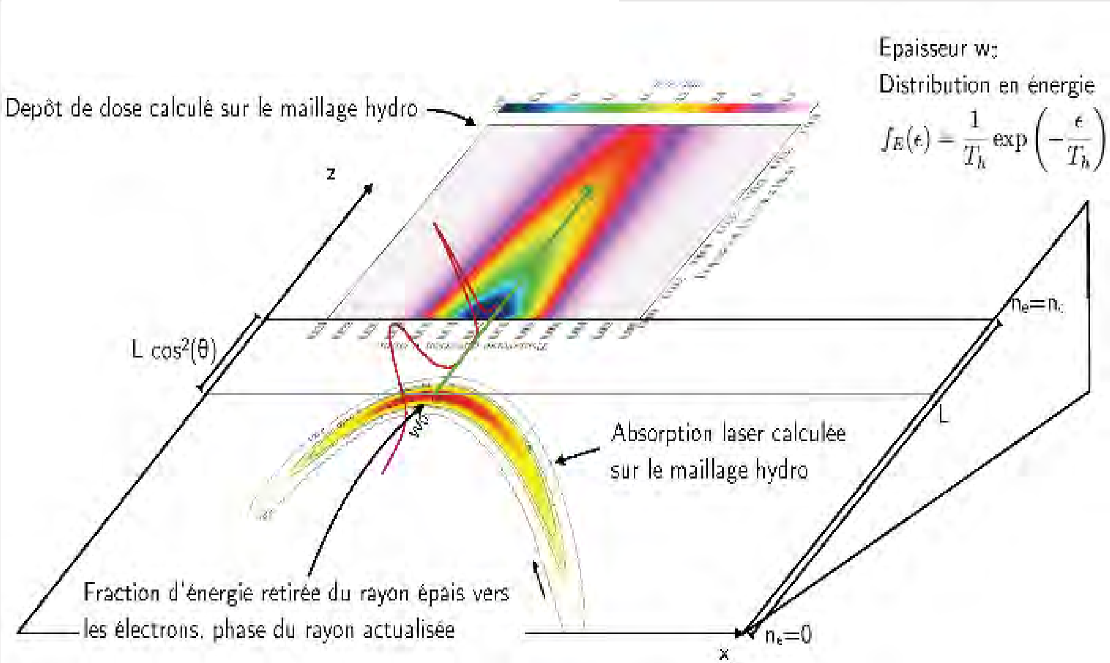

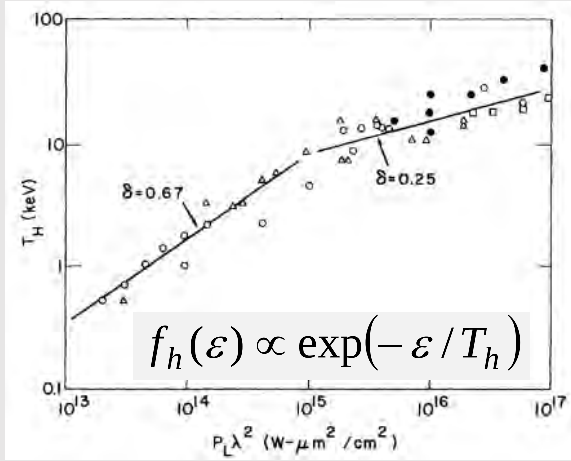

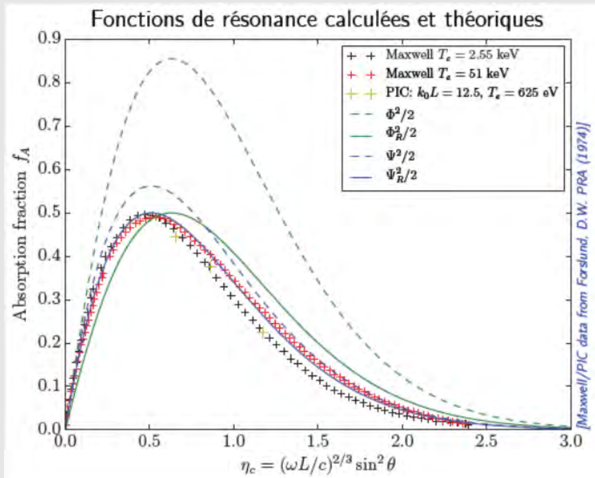

DW Forslund et al, PRA 1974, PRL 1977

The temperature scaling is based on the results of kinetic simulations experimental data

PCGO model of two plasmon decay

The model describes the TPD of each laser beamlet

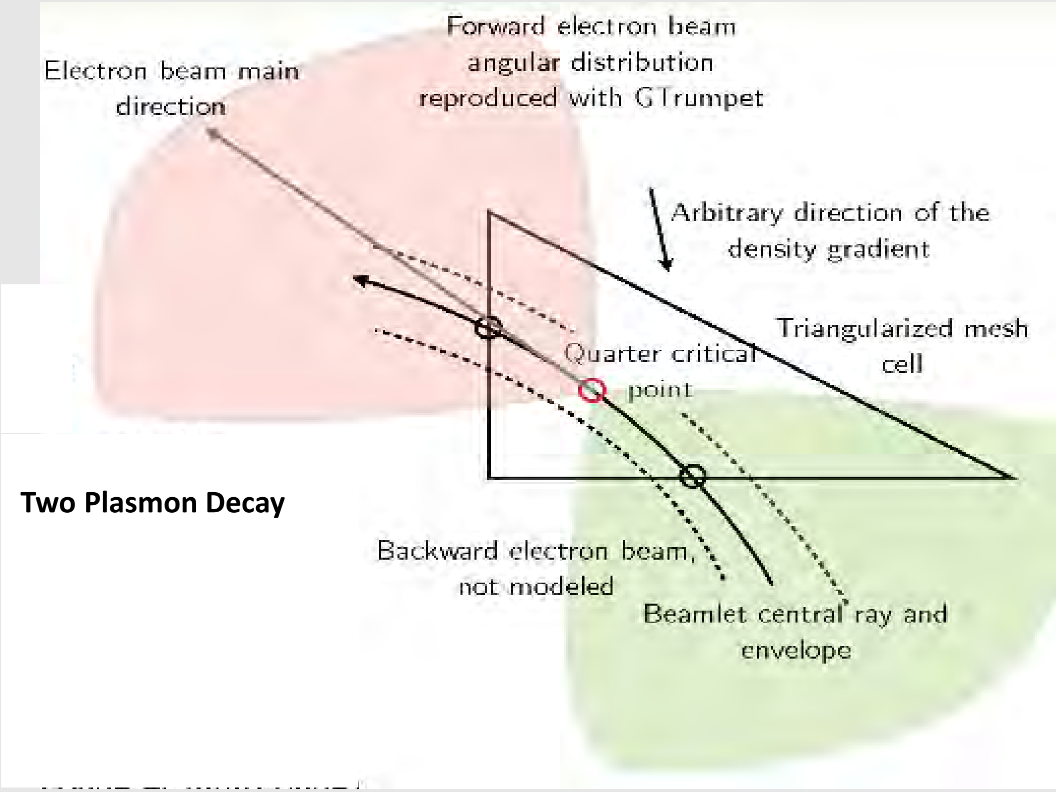

$$T_h = 15.5 + 17.7\, I / I_{th} \ \text{keV}$$

$$\eta_h = 0.026 \left[1 - \exp\left(-\sqrt{I / I_{th} - 1}\right)\right]$$

$$I_{th} = 8.2 T_{\text{keV}} / L_{n\mu\text{m}} \lambda_{\mu\text{m}} \ \text{PW/cm}^2$$

- **Hot electron temperature is not correlated with the phase velocity of the plasma wave because of large spectrum of excited waves**
- **Multistage electron acceleration**
- **Electron emission in the propagation direction of the beamlet**
- **Broad angle emission $\pm 45°$**

The model is based on the results of kinetic simulations and experimental data

R Yan et al, PRL 2012
HX Vu et al, Phys Plasmas 2012

PCGO model of stimulated Raman scattering

The model describes the SRS of each laser beamlet

Stimulated Raman Scattering

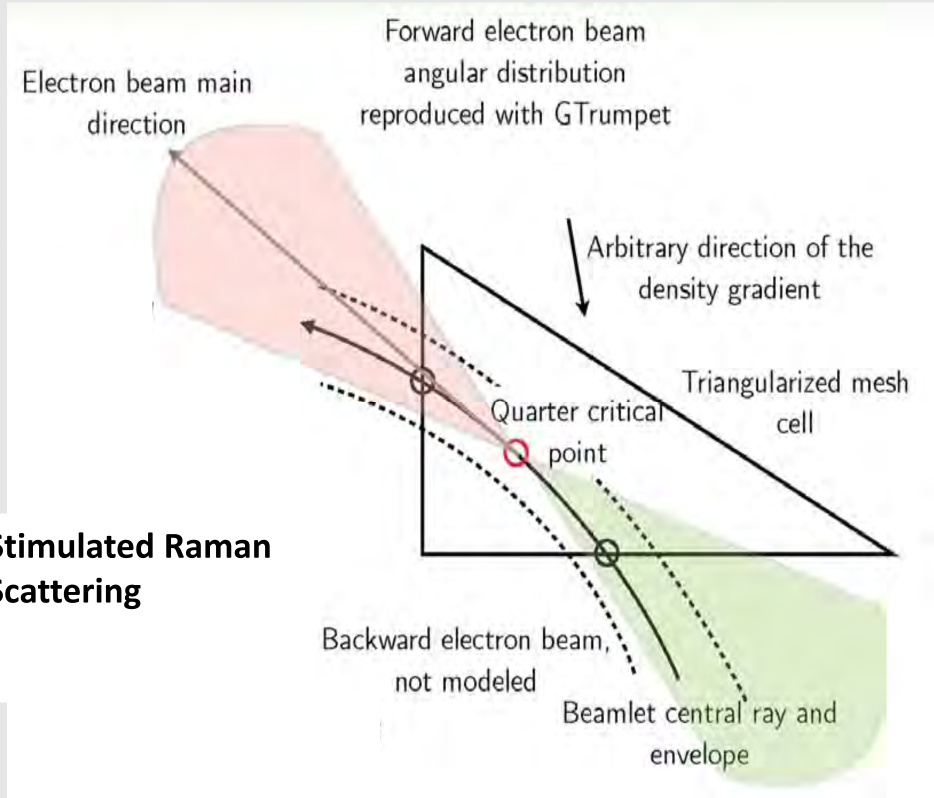

$$T_h = \frac{1}{2} m_e v_{ph}^2$$

$$\eta_h = 0.026 \left[1 - \exp\left(-\sqrt{I / I_{th} - 1}\right)\right]$$

$$I_{th} = 99.5 L_{n\mu m}^{-4/3} \lambda_{\mu m}^{-2/3} \ \text{PW/cm}^2$$

- **Hot electron temperature is correlated with the phase velocity of the plasma wave and depends on the density where SRS is developed**
- **Hot electron number increases with the laser intensity, I/I_{th}**
- **Electron emission in the propagation direction of the beamlet**
- **Narrow angle emission**

The model is based on the results of kinetic simulations and experimental data

O Klimo et al, PPCF 2013, 2014

Modeling of the planar shock experiment

In the PALS experiment the shock pressure was evaluated from the delay of thermal emission from the rear target side

High intensity interaction beam ~ 10^{16} W/cm^2 & 430 nm

pulse duration 300 ps **target areal density ~ 16 mg/cm^2**

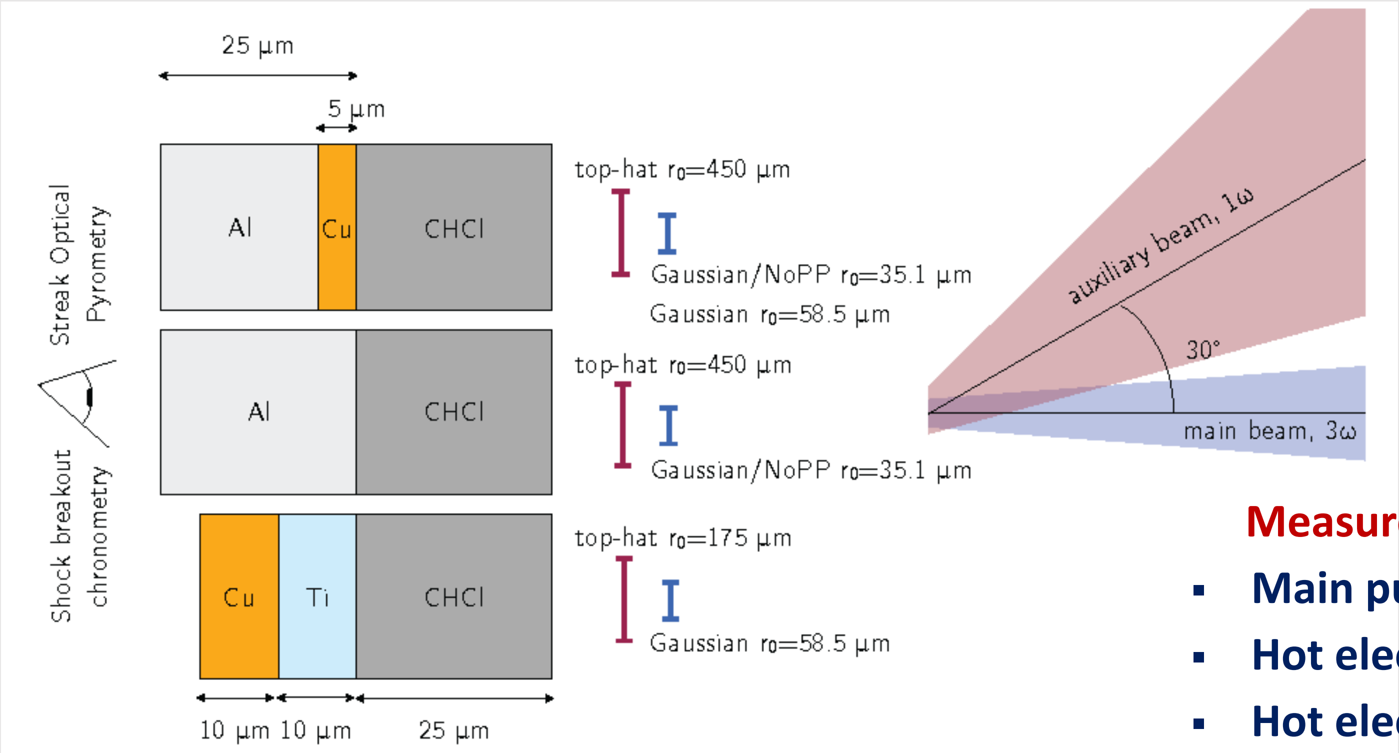

Measured parameters:

- **Main pulse reflectivity**
- **Hot electron temperature**
- **Hot electron flux**
- **Shock breakout time**

Simulations with standard hydrocodes (DUED, MULTI, CHIC) cannot reproduce the measured shock timing

Shock breakout time measurements

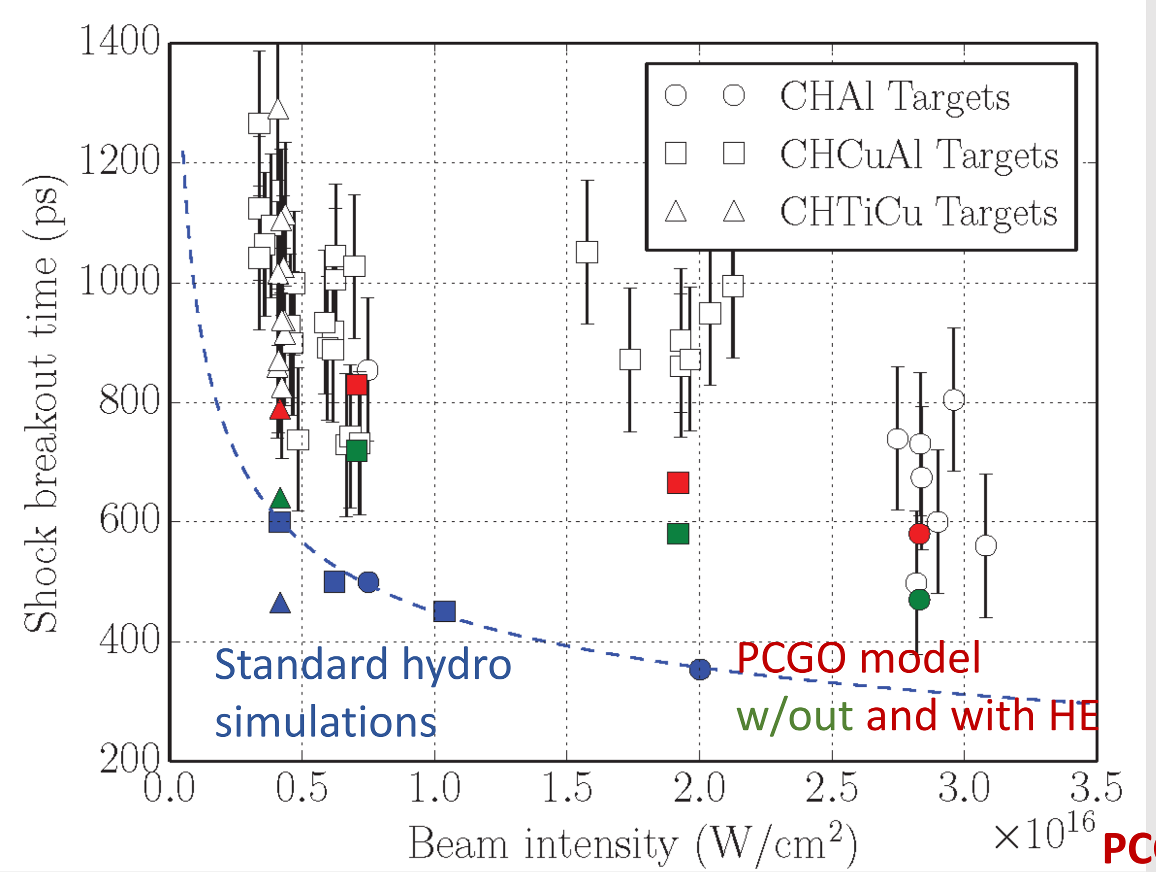

- **PCGO model provides a better timing with the correct laser absorption and hot electron fraction**
- **Explains the role of hot electrons in the shock generation and propagation**

PCGO-HE model

- **Main pulse reflectivity ~ 25%**
- **Hot electron temperature ~ 25-30 keV**
- **Hot electron flux ~ 0.7% of the incident laser energy**

B. Batani et al, Phys Plasmas 2014
Ph. Nicolai et al, Phys Plasmas 2015

Shock propagation simulation

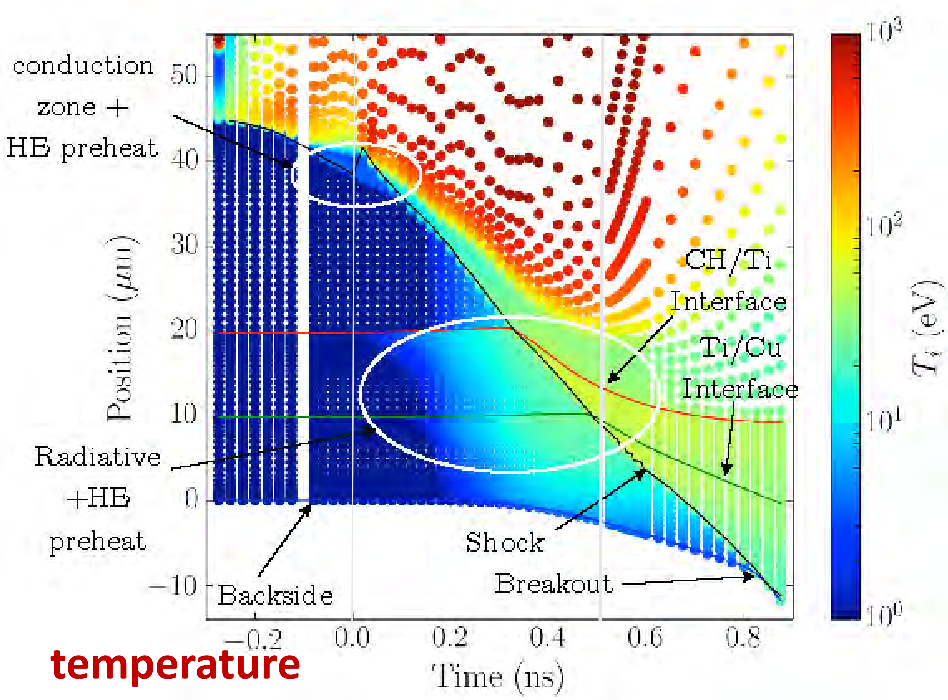

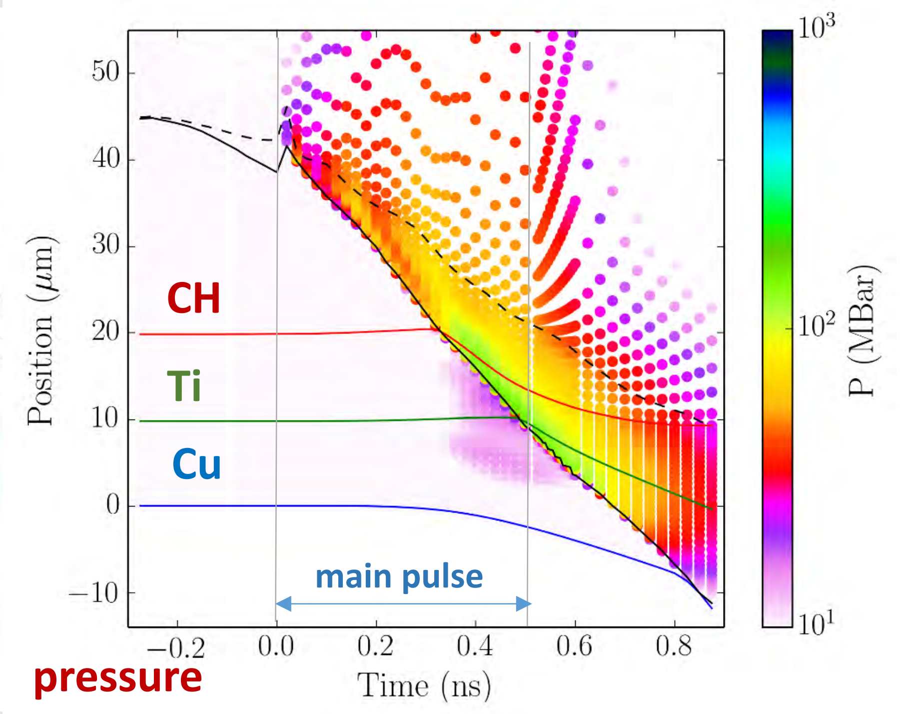

- **Hot electron generation at the beginning of pulse is due to the resonance absorption**
- **Second flash of hot electrons is due to the SRS and TPD – higher energy**
- **Hot electrons increase the shock pressure by less than 30% and accelerate the shock**
- **Hot electrons preheat upstream target to > 10 eV and reduce shock strength by a factor of 10-20**
- **Hot electron preheat initiates the target expansion thus delaying the shock breakout**

OMEGA experiment on strong shock generation

Series of experiments on strong shock generation on the Omega facility in spherical geometry

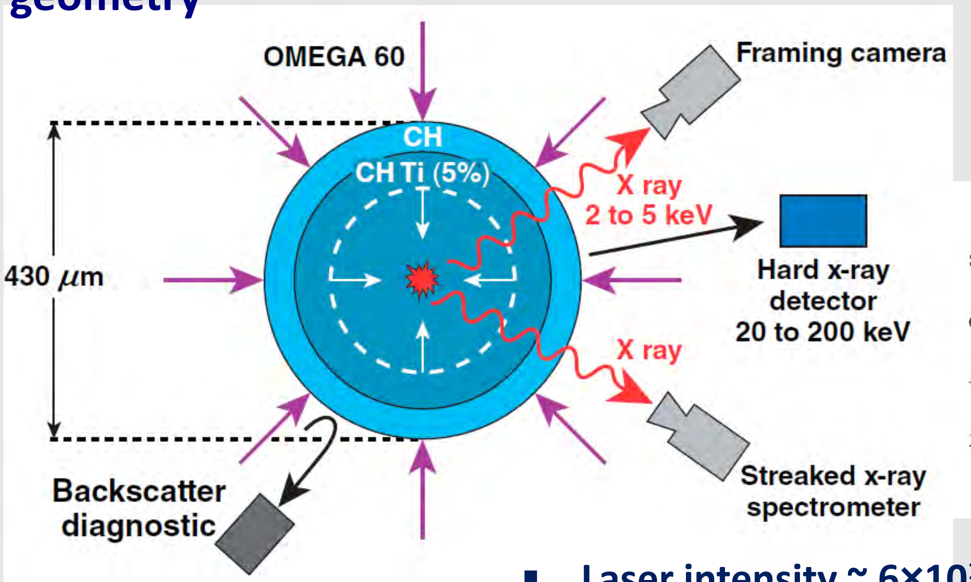

The shock amplitude is evaluated from the measured laser energy absorption and the X-ray flash delay

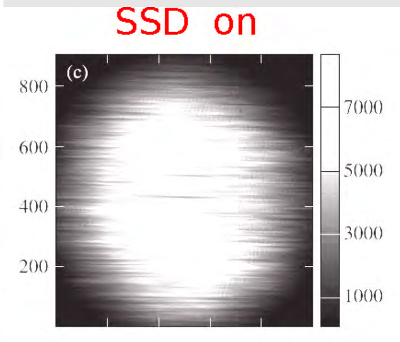

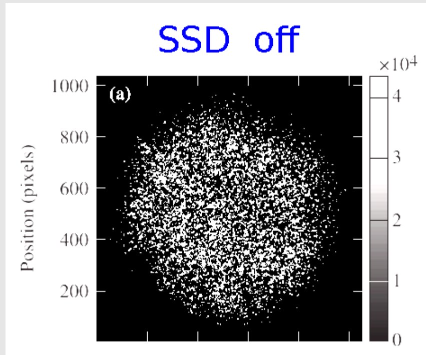

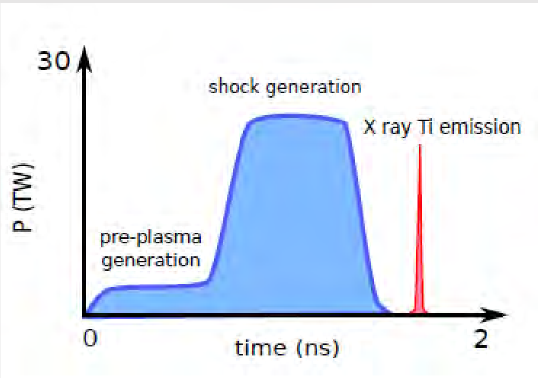

- Laser intensity ~ 6×10^{15} W/cm^2 @ 351 nm
- Measured laser absorption and hot electron number and energy
- Higher local intensities achieved with a non-smoothed laser energy distribution
- Correlation of HE production and SRS
- Stronger shock in the shots with SSD off

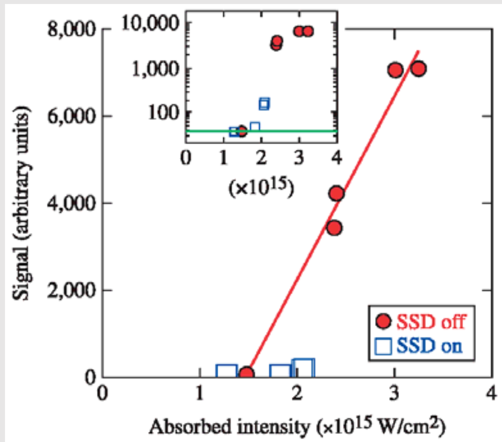

R. Nora et al, Phys Rev Lett 2015
W. Theobald, Phys Plasmas 2015

Correlation between Raman scattering and hot electrons

- The SRS signal is correlated with the number of hot electrons and the laser beam temporal smoothing
- The temperature of hot electrons remains constant

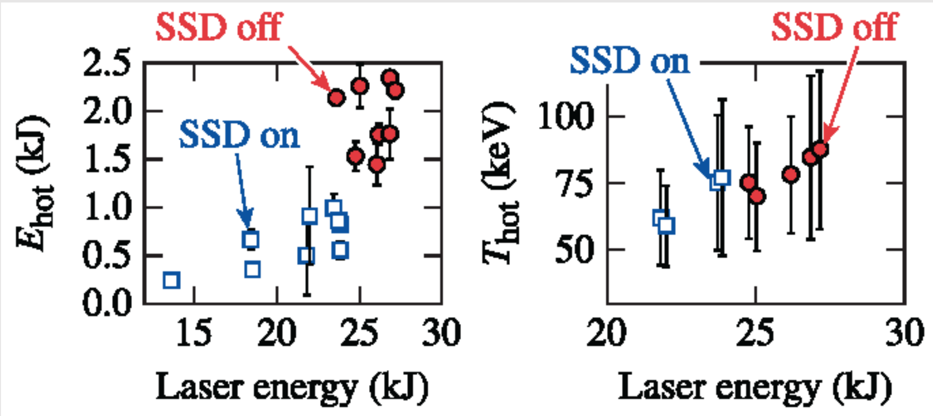

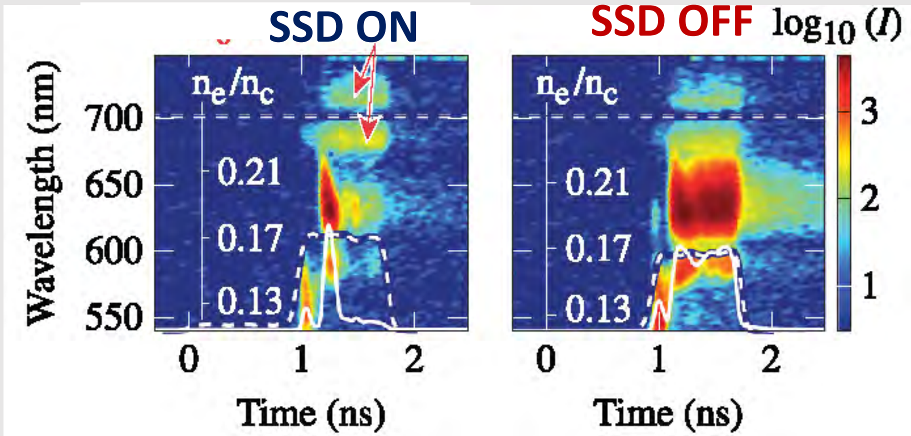

3× higher number of hot electrons for the case w/out SSD

5× stronger SRS signal for the case w/out SSD

Observations are in qualitative agreement with the laser-plasma simulations

W. Theobald, Phys Plasmas 2015

Modeling of the strong shock experiment on OMEGA

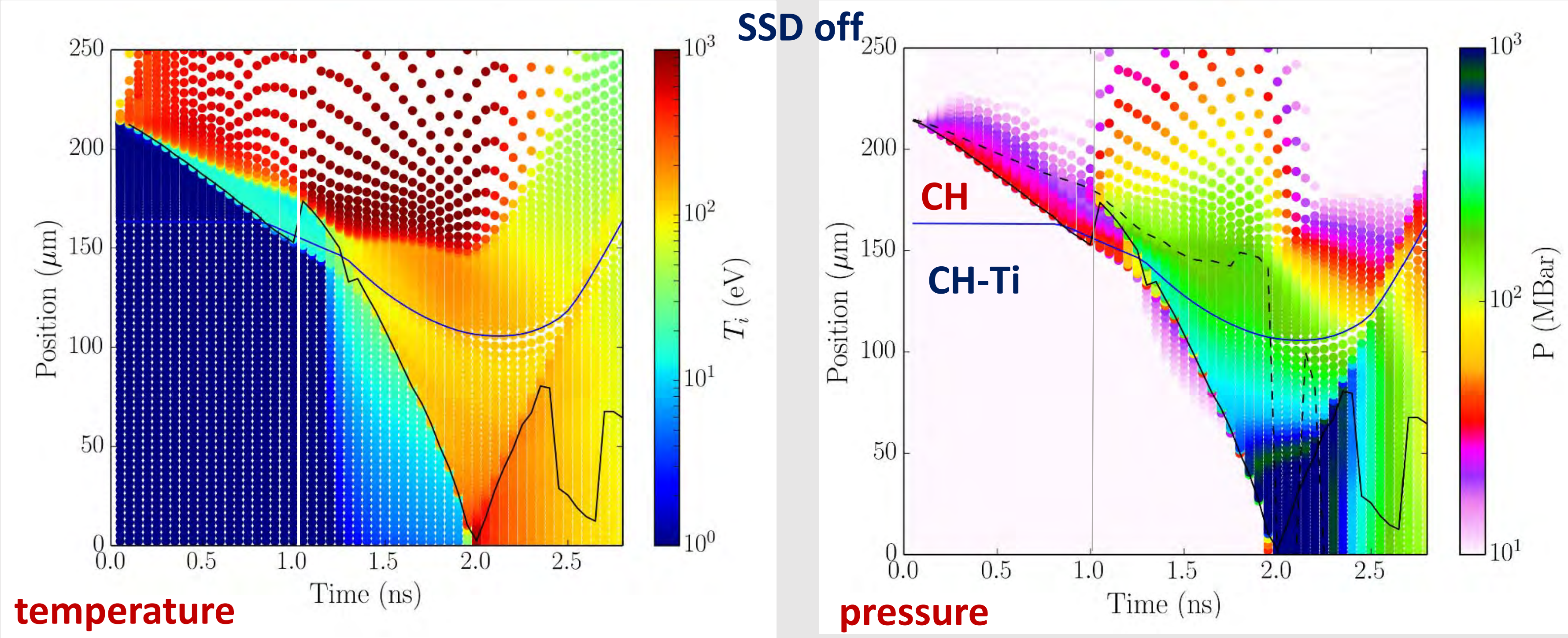

- **PCGO-HE with *C* = 0.6 model reproduces the laser absorption of 56% with a standard flux limiter 4% and the shock flash time 1.98 ns**
- **Collisional absorption of 48%, hot electron fraction 8% agrees with measurements**
- **Hot electrons do not affect the ablation pressure**
- **Hot electrons increase of shock pressure by ~ 50% and increase the shock velocity**
- **Hot electron preheat of upstream target decrease the shock strength by 10-20 times**

α-particle kinetics in the hot spot

Kinetic treatment of the a-particle transport is important for the accurate definition of the ignition threshold and the gain

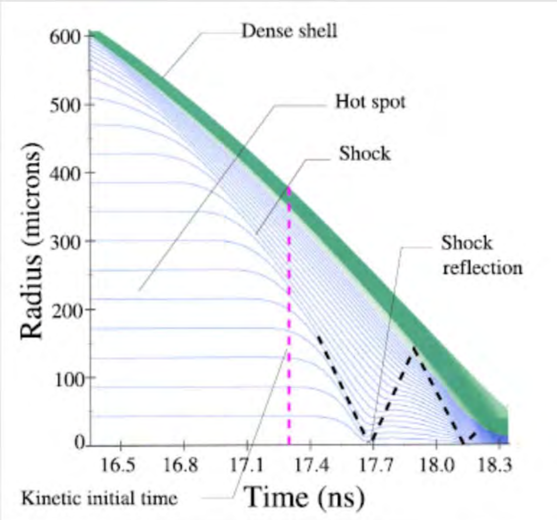

Hybrid – hydrodynamic + ion kinetic simulation of the standard NIF target:

- **Earlier ignition**
- **Lower fusion yield**
- **Deep penetration of α–particles in shell**
- **Broader burn front**

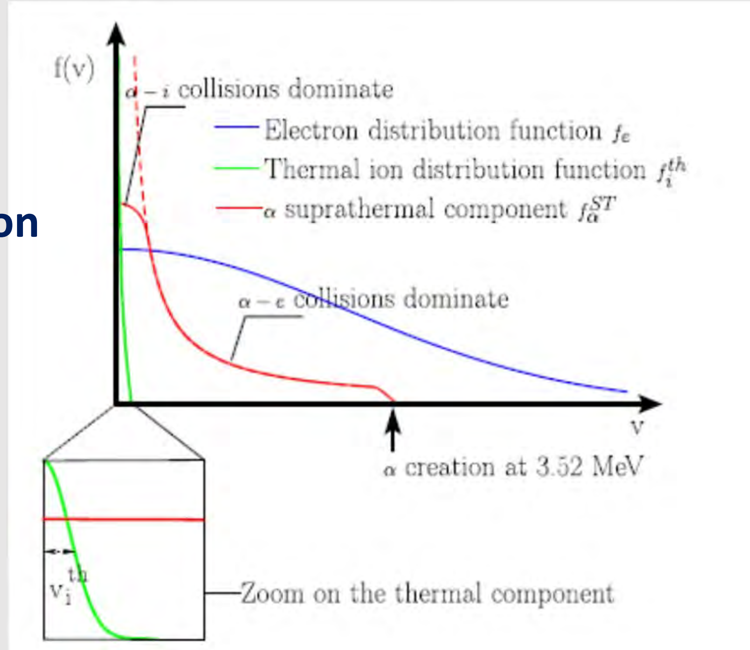

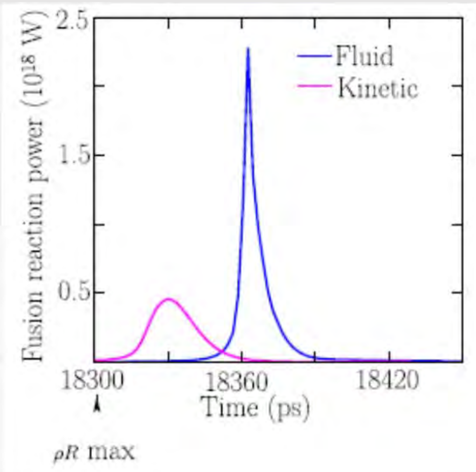

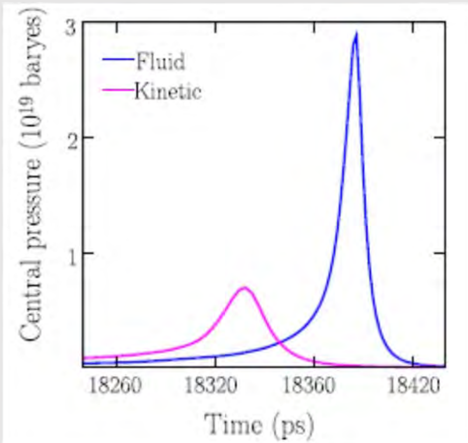

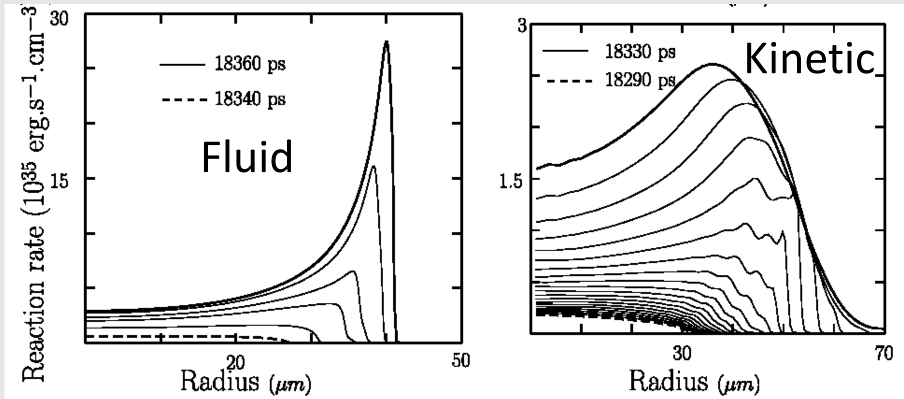

B Peigney et al, Phys Plasmas 2014

Conclusions – perspectives

- **Shock Ignition is the alternative ICF approach, which requires less laser energy and is compatible with the existent megajoule facilities NIF and LMJ**
- **Laser spike intensity ~ 10 PW/cm^2 implies strongly nonlinear laser plasma interaction conditions and hot electron generation**
- **Shock pressure ~ 30 Gbar is required for the hot spot ignition, it can be achieved by 100$\times$ amplification of the shock in the imploding shell**
- **PCGO-HE model is tested in the OMEGA and PALS experiments showing: increase of the shock pressure and velocity, strong decrease of the shock strength. Protection of the shell and the hot spot from the hot electron preheat has to be considered in the SI target design**
- **Contribution of hot electrons is indispensable for achieving Gbar pressures. It opens new horizons for material studies at extreme conditions**

First academic experiments on the LMJ-PETAL facility are planned for 2018

Strong shock generation experiment is selected by the Selection Committee